Sustainable Chemical Engineering
http://ojs.wiserpub.com/index.php/SCE/

UNIVERSAL WISER PUBLISHER

Research Article

Evaluating the Potential of Modified Mango Leaves as a Biosorbent for the Removal of Mercury (II) Ion and Congo Red from Wastewater

Oluwaseun Adekoya Adelaja[1], Babafemi Raphael Babaniyi[2*]

[1]Department of Chemistry, School of physical sciences, Federal University of Technology Akure, Nigeria
[2]Bioresources Development Centre, National Biotechnology Development Agency, Nigeria
Email: babafemiraphael@gmail.com

Received: 30 April 2024; **Revised:** 17 June 2024; **Accepted:** 21 June 2024

Abstract: The discharge of harmful metallic elements from industrial byproducts has resulted in notable environmental and public health risks. The aim of this study was to investigate the effectiveness of mango leaves as a cost-effective adsorbent in eliminating Hg (II) ions from industrial effluents. Experimental procedures were carried out under controlled conditions at ambient temperature to evaluate the influence of pH, contact duration, initial metal levels, adsorbent quantity, and temperature on the adsorption mechanism. The most favorable pH for optimal Hg (II) ions adsorption was identified at pH 7. The adsorption process displayed swift kinetics in the initial 30 minutes of contact, leading to a removal rate exceeding 90%, with equilibrium achieved after 70 minutes of stirring. Analysis of kinetics revealed a significant correlation coefficient for a pseudo-second-order kinetic equation. The absorption of Hg (II) ions escalated with increased stirring intensity and decreased adsorbent amount. The interaction between Hg (II) ions, Congo red, and mango leaves was analyzed employing Langmuir, Freundlich, and BET isotherm models. The equilibrium data was best fitted by the Langmuir model, presenting a correlation coefficient of 0.98 and a maximum adsorption capacity of 28.40 mg/g. These results underscore the potential of mango leaves as an affordable bio adsorbent for addressing heavy metal pollution in wastewater.

***Keywords*:** modified mango leaves, biosorbent, mercury (II) Ion, congo red, wastewater

1. Introduction

Water pollution arising from the presence of heavy metals and dyes has become a significant environmental issue globally. Among the various heavy metals, mercury (II) ions are particularly concerning due to their harmful effects on human health, animals, and aquatic organisms.[1] In a similar vein, Congo red dye, commonly used in the textile industry, has been recognized as a dangerous pollutant because of its cancer-causing and mutation-inducing properties.[2] Traditional methods like precipitation, coagulation, and membrane filtration, commonly used to remove these pollutants from wastewater, are often expensive and inefficient, especially with low pollutant concentrations.[3]

Biosorption, an eco-friendly and cost-efficient method, involves using natural or synthetic materials to eliminate contaminants from wastewater.[4] Mango leaves, which are abundant in tropical areas, are a potentially effective biosorption material due to their various functional groups that can interact with pollutants. The biosorption capabilities and selectivity of mango leaves can be enhanced through chemical alterations.[5] Several research studies have

DOI: https://doi.org/10.37256/sce.5220244854

investigated the biosorption of mercury (II) ions and Congo red dye using different adsorbents, including mango leaves.[6] For example, Liu et al.[7] studied the biosorption of mercury (II) from water solutions using modified mango leaves and observed a significant increase in adsorption capacity post-modification. Muhulet et al.[8] looked into the biosorption of Congo red dye with both untreated and treated mango leaves, finding that treated mango leaves had higher adsorption capacity and faster rates of adsorption. Similarly, Wang et al.[9] explored the biosorption of mercury (II) using mango leaves modified with polyethyleneimine, determining that modified mango leaves had superior adsorption capacity compared to untreated ones. Devi and Saroha[10] investigated the biosorption of mercury (II) ions using activated carbon derived from mango leaves and discovered that the activated carbon had a high adsorption capacity, effectively eliminating mercury (II) ions from water solutions.

Fazlzadeh et al.[11] investigated the removal of Congo red dye using activated carbon derived from magnetically modified mango leaves. They observed a significant increase in adsorption capacity following magnetic modification, and the adsorbent effectively removed Congo red from aqueous solutions. Kumar and Kumar[12-13] examined the biosorption of Congo red dye using acid-treated mango leaf powder, finding that the adsorption capacity increased after acid treatment, enabling effective dye removal.

These studies highlight the potential of mango leaves and their derivatives as effective adsorbents for removing mercury (II) ions and Congo red dye from wastewater. However, there is a lack of comprehensive research on the biosorption of both mercury (II) ions and Congo red dye using chemically altered mango leaves treated with potassium persulfate. Further research is needed to optimize biosorption conditions for single and mixed contaminant solutions. The specific modification technique involving potassium persulfate has not been extensively explored for the biosorption of both pollutants.

Potassium persulfate, a strong oxidizing agent used in polymer fabrication and as a bleaching agent, can introduce functional groups onto adsorbent surfaces, enhancing adsorption capacity and selectivity. This study aims to address research gaps and provide a detailed understanding of the biosorption of mercury (II) ions and Congo red dye using chemically modified mango leaves.

The primary objective is to investigate the biosorption process for removing mercury (II) ions and Congo red dye from wastewater with chemically modified mango leaves. This study will offer insights into the mechanisms of biosorption and the factors affecting the adsorption capacity and selectivity of mango leaves. Optimal conditions for biosorption, including pH levels and temperature, will be determined to evaluate the efficacy of the chemically modified mango leaves. The results will contribute to developing a sustainable and cost-effective method for pollutant removal from wastewater, leveraging the abundant availability and reusability of mango leaves in tropical regions.

2. Experimental

2.1 *Chemicals and reagents*

The chemical substances used in this investigation included Congo red dye, mercury (II) chloride, potassium persulfate, sodium hydroxide (NaOH), hydrochloric acid (HCl), diphenyl thiocarbazone, 1,4-dioxane, and triple-distilled water. Primary solutions were prepared by dissolving mercury (II) chloride and potassium persulfate in triple-distilled water to a concentration of 1,000 mg/L. Secondary standard solutions were then made from these primary solutions, with pH adjustments using 0.1 M HNO_3 and 0.1 M NaOH.

2.2 *Preparation of mango leaves for adsorption process*

2.2.1 *Adsorbent collection and preparation*

Mango leaves were collected from the Federal University of Technology Akure (FUTA) campus, Ondo State, Nigeria. Leaves without blemishes were thoroughly cleaned with distilled water to remove soluble substances and particulate matter. An acidic rinse with 0.01 M HCl was performed to remove additional impurities, followed by another distilled water rinse. The leaves were then sun-dried for three days to remove excess moisture, and subsequently oven-dried at 105 °C for three hours to ensure complete moisture removal. The dried leaves were pulverized using a Willey mill and sieved through a 250 µm mesh to obtain a uniform particle size, which was then stored in an airtight container.

2.2.2 *Pre-treatment of the adsorbent*

According to Xue et al.[14] 75 grams of pulverized mango leaves were combined with 40 grams of potassium persulfate dissolved in 200 mL of distilled water in a beaker. After adding an additional 200 mL of distilled water, the mixture was stirred and allowed to sit at room temperature (30.5 °C) for two hours. The mixture was then rinsed with distilled water, transferred to a crucible, and heated at 80 °C in an oven. Once dried, it was ground using a mortar and pestle and stored in an airtight container. This preparation and modification process ensured that the adsorbent was effective in removing mercury (II) ions and Congo red dye from wastewater.

2.3 *Experimental design for adsorption process*

2.3.1 *Effect of pH*

The impact of pH on the sorption of Congo red dye, mercury (II) chloride ions, and their combined mixture utilizing pre-treated mango leaves powder was examined. Within each trial, 0.1 g of the sorbent was introduced to six containers holding 1.5 mL of a 60 mg/L solution of the sorbate and 48.3 mL of wastewater. The pH levels were modified from 4.0 to 9.0 through the utilization of 0.1 M HCl and 0.1 M NaOH. The samples underwent agitation for a duration of 2 hours at 100 rpm, and the liquid above the sediment was assessed for light absorption at 497 nm for Congo red and 488 nm for mercury (II) chloride utilizing a UV-VIS spectrophotometer. In the scenario of the combined mixture, 1.5 mL of a 60 mg/L solution for each sorbate was combined in the container alongside 46.8 mL of wastewater, and light absorption was evaluated in a similar manner.

2.3.2 *Effect of contact time*

The impact of contact duration on the process of adsorption was investigated utilizing mango leaves powder that had undergone pretreatment. Within each trial, 0.1 g of the adsorbent substance was combined with the corresponding solution in five separate vessels, standardized to a pH of 7, and subjected to agitation at varying time intervals (25, 50, 75, 100, 125 minutes). Subsequent to the agitation, the solution containing the dye was sieved, and the level of light absorption of the resulting liquid was gauged at wavelengths of 497 nm for Congo red and 488 nm for mercury (II) chloride. In the case of the mixture comprising two substances, 1.5 mL of each solution was introduced into the vessel alongside 46.8 mL of wastewater, and the level of absorption was quantified following the established procedure.

2.3.3 *Effect of adsorbent dosage*

Various quantities of pre-treated mango leaf powder (0.05, 0.1, 0.15, 0.2, 0.25 g) were employed in the examination of the impact of adsorbent dosage. Each specific quantity was blended with 1.5 mL of a 60 mg/L solution of Congo red dye or a 1.5 mL solution of 60 mg/L mercury (II), adjusted to a pH of 7, and stirred for the optimal duration of contact. The optical density of the resulting liquid was gauged utilizing a UV-VIS spectrophotometer at 488 nm for mercury (II) and 497 nm for Congo red.

2.3.4 *Effect of initial concentration*

The effect of initial concentration on the removal efficiency of Congo red dye and mercury (II) chloride ions was studied using different initial concentrations (30, 60, 90, and 120 mg/L). For the binary mixture, different initial concentrations of both dye and ions were used, and the samples were adjusted to pH 7 and shaken for 2 hours. Absorbance was measured at 497 nm for Congo red and 488 nm for mercury (II) ions using a UV-visible spectrophotometer.

2.3.5 *Thermodynamic studies*

The effect of temperature on the adsorption process was examined using pretreated mango leaves. For Congo red dye and mercury (II) ions, 0.1 g of adsorbent was added to 6 beakers with 1.5 mL of 60 mg/L dye or ion solution and 48.3 mL of wastewater. Samples were agitated for 2 hours at temperatures ranging from 30 to 70 °C, and absorbance

was measured at 497 nm for Congo red and 488 nm for mercury (II) ions. For the binary mixture, the procedure was similar, with 1.5 mL of each solution and 46.8 mL of wastewater.

2.4 *Adsorption kinetics*

The adsorption kinetics of Congo red dye and mercury (II) chloride ions were studied using pretreated mango leaves. For Congo red dye, 0.1 g of adsorbent was added to beakers containing 3 mL of 120 mg/L dye concentration in wastewater, adjusted to pH 7, and agitated at different time intervals (25, 50, 75, 100 mins). The supernatant was measured at 497 nm. For mercury (II) chloride ions, a similar procedure was followed using 3 mL of 120 mg/L mercuric chloride concentration. For the binary mixture, 3 mL of each solution was added to beakers containing 0.1 g of adsorbent, adjusted to pH 7, and agitated at different time intervals.[15]

3. Results and discussion

3.1 *Optimization of factors affecting the adsorption of congo red dye, mercury (ii), and their binary mixture*

3.1.1 *Effect of pH*

The influence of pH on the removal of Congo red dye, mercury (II) ions, and their combined removal was investigated across a pH range of 4 to 9. Figure 1 provides an overview of the percentage removal efficiency at various pH levels.

Congo Red Dye: The removal efficiency of Congo red dye declined from 65.95% at pH 4 to 55.96% at pH 9. This reduction is attributed to two main factors:

(1) Increased Protonation at Lower pH Levels: At lower pH, the adsorbent surface becomes more protonated, enhancing the binding of the anionic dye to the adsorbent's carbon surface.

(2) Competition at Higher pH Levels: At higher pH, negatively charged ions such as SO_4^{2-} and $H_2SO_4^-$, resulting from the reaction between hydroxyl ions from 0.1 M NaOH and $S_2O_8^{2-}$ used in mango leaves modification, compete with the anionic dye for sorption sites.

These findings align with prior research by Sathya et al.[16] and other studies that reported a decrease in Congo red dye removal efficiency with increasing pH.[17-18] The reduced removal efficiency at higher pH is also due to the ionization of functional groups on the adsorbent's surface, diminishing the electrostatic attraction between the adsorbent and dye molecules.[19]

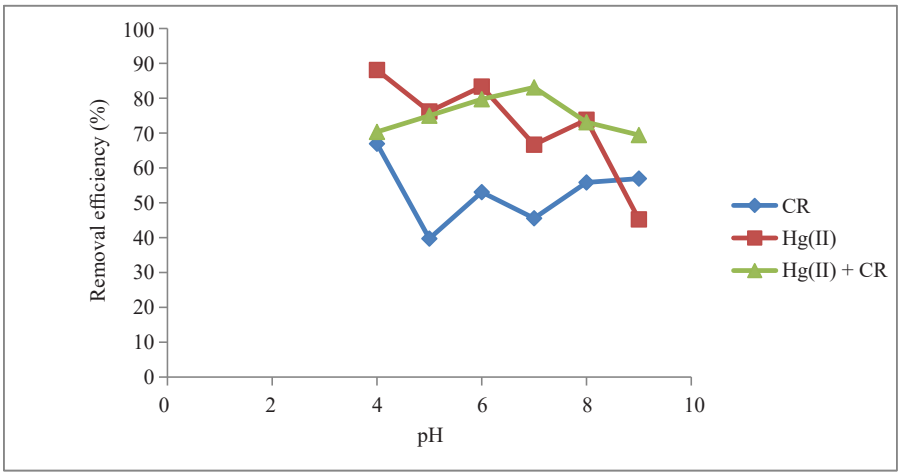

Figure 1. Effect of pH on removal of Congo red dye, mercury (II) ions and their binary mixture. Initial concentration = 60 mg/l, Agitation speed = 100 rpm, Contact time = 2 hours, Adsorbent dosage = 0.1 g, Hg (II) = Mercury (II) ion and CR = Congo red dye and Hg (II) + CR = mercury (II) ions and Congo red dye

Mercury (II) Ions: The removal efficiency of mercury (II) ions decreased as pH levels increased. Specifically, the removal percentage decreased from 87.2% at pH 4 to 45.35% at pH 9. The optimal pH for mercury (II) ions adsorption by modified mango leaves was found to be 4. This can be attributed to the presence of negatively charged ions on the adsorbent surface, such as SO_4^{2-} formed from potassium persulfate and Cl^- from both 0.1 M hydrochloric acid and mercuric chloride. These ions form complexes with Hg^{2+}, enhancing the adsorption at its maximum capacity.

As pH increased, the removal efficiency decreased due to competition with other positively charged ions like $K^+$from potassium persulfate and H^+ from 0.1 M hydrochloric acid, leading to reduced adsorption efficiency.[16] Notably, at pH 6 and 8, the removal efficiency was 83.10% and 73.81%, respectively. This indicates increased efficiency at these levels due to the stronger affinity of negatively charged ions for Hg^{2+} compared to other positive ions. This pattern aligns with previous studies showing that mercury (II) ions removal efficiency generally increases with rising pH up to a certain point before decreasing due to complex species formation or precipitation.[20-21]

Binary Mixture of Congo Red Dye and Mercury (II) Ions: The removal efficiency for both pollutants increased as pH levels rose from 4 to 7 and then declined as pH continued to increase to 9. This trend is consistent with previous research findings.[22-23] The decrease in removal efficiency for the binary mixture can be attributed to competitive adsorption between the two pollutants, which reduces the available adsorption sites for each.[24]

3.1.2 *Effect of contact time*

As depicted in Figure 2, the sorption rate of Congo red dye increases with contact time. This is due to the abundance of binding sites, including K^+ from $K_2S_2O_8$, Na^+ from NaOH, and H^+ from HCl, on the modified mango leaves, which facilitate the dye's adsorption in the wastewater. Equilibrium is reached at 120 minutes, when the binding sites become saturated, and the removal rate slows down due to the reduced availability of active sites.[25]

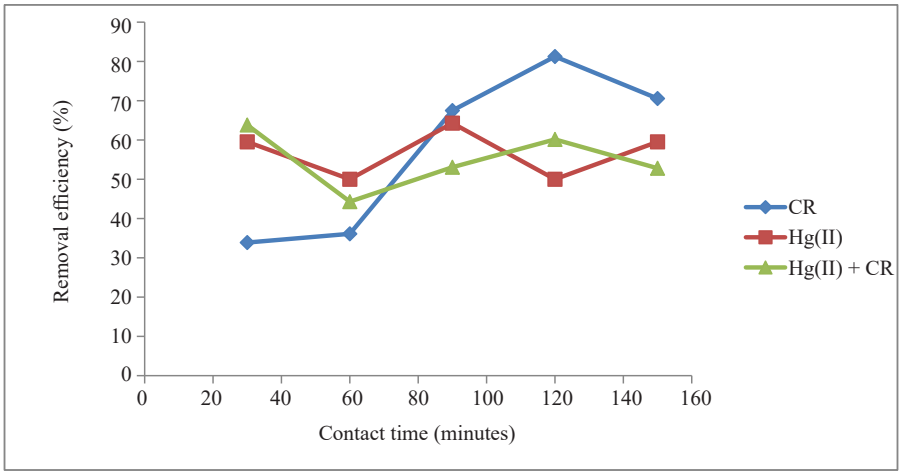

Figure 2. Effect of contact time on removal of Congo red dye, mercury (II) ions and their binary mixture. pH = 7, Initial concentration = 60 mg/L, Agitation speed = 100 rpm, Adsorbent dosage = 0.1 g, Hg (II) = Mercury (II) ion and CR = Congo red dye and Hg (II) + CR = mercury (II) ions and Congo red dye

For mercury (II) ions, the percentage removal initially increases but then decreases due to interference from competing ions like K^+, Na^+, and H^+. Equilibrium is reached at 90 minutes, followed by a decline in removal efficiency as the active sites are depleted by 120 minutes. Interestingly, at 150 minutes, there is an upswing in mercury (II) ion removal, possibly due to the reavailability of active sites.[26]

In the case of the binary mixture of Congo red dye and mercury (II) ions, the removal efficiency declines with increasing contact time due to the scarcity of sorption sites. At the 30-minute mark, the adsorbent removes 63.8% of the binary mixture, indicating this as the optimum contact time due to the ample surface area available. Similar observations have been documented in prior studies.[27-28]

3.1.3 *Effect of adsorbent dosages*

The impact of adsorbent dosages, ranging from 0.05 g to 0.25 g, on the adsorption of Congo red dye, mercury (II) ions, and their binary mixture is depicted in Figure 3. As the adsorbent dosage increased, there was a corresponding rise in the amount of Congo red dye adsorbed due to the expansion of the adsorbent's surface area, which augments the number of available binding sites. This observation aligns with previous studies, such as Sharma et al.[29] who found that increasing the adsorbent dosage from 0.05 g to 0.25 g led to higher removal of Congo red dye using orange peel as the adsorbent. Figure 3 shows that the adsorption of Congo red dye increased from 33.85% to 57.09% as the adsorbent dosage rose from 0.05 g to 0.25 g.

However, at an adsorbent dosage of 0.2 g, there was a noticeable drop in the percentage removal. This reduction was due to the overlapping of adsorption sites, a phenomenon supported by the findings of Wang et al.[30] who observed a decrease in the removal efficiency of Congo red dye with an increase in the adsorbent dosage of modified starch.

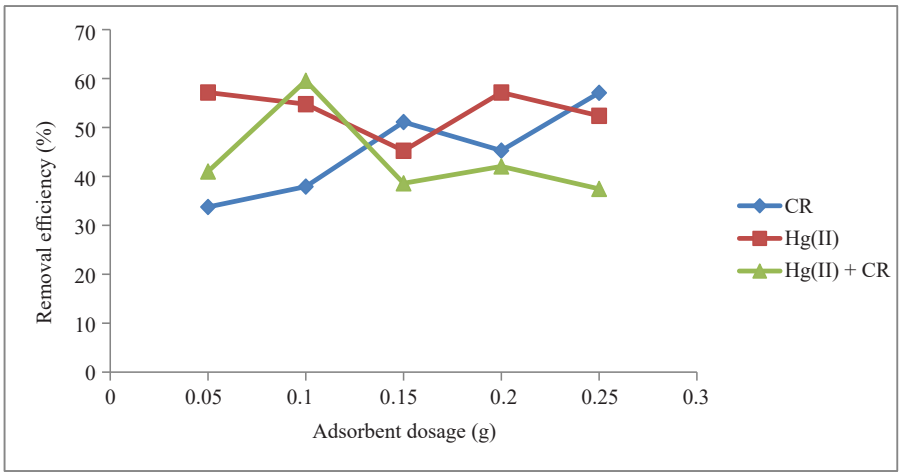

Figure 3. Effect of the adsorbent dosage on removal of Congo red dyes, mercury (II) ions and their binary mixture. pH = 7, Initial concentration = 60 mg/L, Agitation speed = 100 rpm, Contact time = 2 hrs 10 minutes, Hg (II) = Mercury (II) ion and CR = Congo red dye and Hg (II) + CR = mercury (II) ions and Congo red dye

In Figure 3, an increase in the adsorbent dosage led to a decrease in the affinity of mercury (II) ions to bind with the available sites, attributed to the overlapping of negatively charged ions on the surface.[31] Subsequently, the percentage removal increased with higher dosage until reaching equilibrium at 0.2 g, with a removal efficiency of 57.14%. This equilibrium resulted from the depletion of available binding sites, consistent with Zhou et al.'s findings.[32] However, at higher dosages, efficiency declined due to site saturation, leading to a gradual decrease in removal percentage.

For the binary mixture, introducing both mercury (II) ions and Congo red dye affected the adsorption process as the dosage increased. The optimal dosage was 0.1 g, minimizing site overlap and resulting in a 59.56% removal rate. This finding aligns with Wang et al.'s observations[33] on binary dye mixture removal efficiency with increasing adsorbent dosage.

3.1.4 *Effect of the initial concentration*

Figure 4 illustrates the impact of initial concentration, ranging from 30 to 120 mg/L, on the adsorption of Congo red dye, mercury (II) ions, and their binary mixture. As the initial concentration of Congo red increased, the percentage removal decreased from 35.6 mg/g to 22.1 mg/g. However, the amount of Congo red dye sorbed per unit mass of modified mango leaves increased from 5.33 mg/g to 13.25 mg/g.

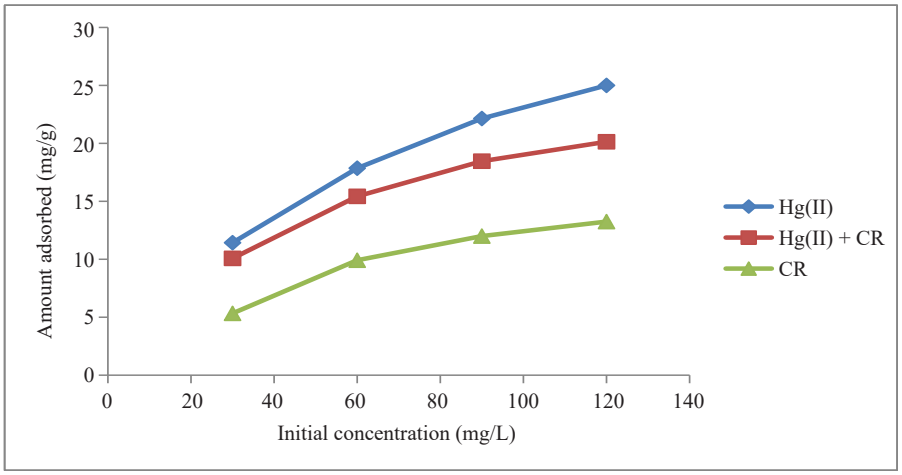

Figure 4. Effect of the initial concentration on removal of Congo red dyes, mercury (II) ions and their binary mixture. pH = 7, Agitation speed = 100 rpm, Contact time = 30 minutes, Adsorbent dosage = 0.1 g, Hg (II) = Mercury (II) ion, CR = Congo red dye and Hg (II) + CR = mercury (II) ions and Congo red dye

This discrepancy suggests that while the percentage removal decreased at higher concentrations due to limited adsorption sites, the absolute quantity of Congo red dye adsorbed per unit mass of the adsorbent increased. Similarly, for mercury (II) ions, the amount adsorbed increased with concentration, while removal efficiency decreased from 76.2 mg/g to 41.67 mg/g. At lower concentrations, mercury (II) ions are primarily bound with available negatively charged ions on the surface, reaching their adsorption capacity limit as concentrations rose, leading to decreased removal efficiency. In the case of the binary mixture, removal efficiency decreased from 67.2 mg/g to 33.56 mg/g with increasing concentration due to binding site exhaustion and competition among similarly charged ions. The study highlighted that mercury (II) ions' adsorption was more efficient than that of the binary mixture and Congo red dye by modified mango leaf powder.

3.2 *Adsorption isotherms*

3.2.1 *Langmuir isotherm*

Figure 5 illustrates the Langmuir isotherm model graph, depicting a linear relationship between C_e/q_e and C_e. This model was employed to characterize the sorption of Hg^{2+} ions, Congo red dye, and their binary mixture onto modified mango leaves.

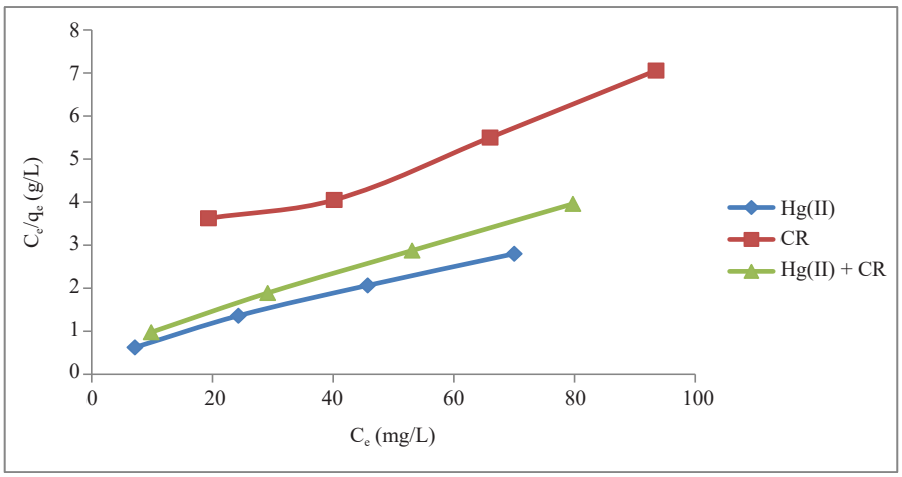

Figure 5. Langmuir isotherm plot for the sorption of mercury (II) ions, Congo red dye and their binary mixture onto modified mango leaves. Hg (II) = Mercury (II) ion and CR = Congo red dye and Hg (II) + CR = mercury (II) ions and Congo red dye

Table 1. Langmuir isotherm parameter

Mercury (II) ions		Congo red dye		Binary mixture	
q_{max}	K_L	q_{max}	K_L	q_{max}	K_L
29.43	0.075	21.45	0.019	24.86	0.070

Table 2. R_L values for the adsorption of mercury (II) ions, Congo red dye and their binary mixture

Initial concentration (mg/L)	Mercury (II) ions R_L	Congo red dye R_L	Binary mixture R_L
30	0.33	0.64	0.32
60	0.18	0.46	0.19
90	0.13	0.37	0.16
120	0.12	0.32	0.13

The equilibrium data for the adsorption of mercury (II) ions, Congo red dye, and their binary mixture onto modified mango leaves powder align most closely with the Langmuir isotherm model, as indicated by the regression coefficients and separation factors (*RL*) falling within the range of 0 to 1. Notably, among these sorbents, mango leaves modified with potassium persulfate exhibited the highest adsorption capacity for mercury (II) ions (q_m = 29.43 mg/g), surpassing the capacities for Congo red dye (q_m = 21.45 mg/g) and their binary mixture (q_m = 24.86 mg/g) (refer to Table 1 and 2). This observation suggests that the Langmuir isotherm model best describes the sorption of mercury (II) ions, indicating their adsorption onto the surface of modified mango leaves in a monolayer pattern characteristic of chemisorption.[34]

3.2.2 *Freundlich isotherm*

The Freundlich isotherm assumes a heterogeneous surface with a non-uniform distribution of biosorption heat and allows for multilayer biosorption. It is represented by the equation:

$$\log q_e = \log K_F + 1/n \log C_e \quad (1)$$

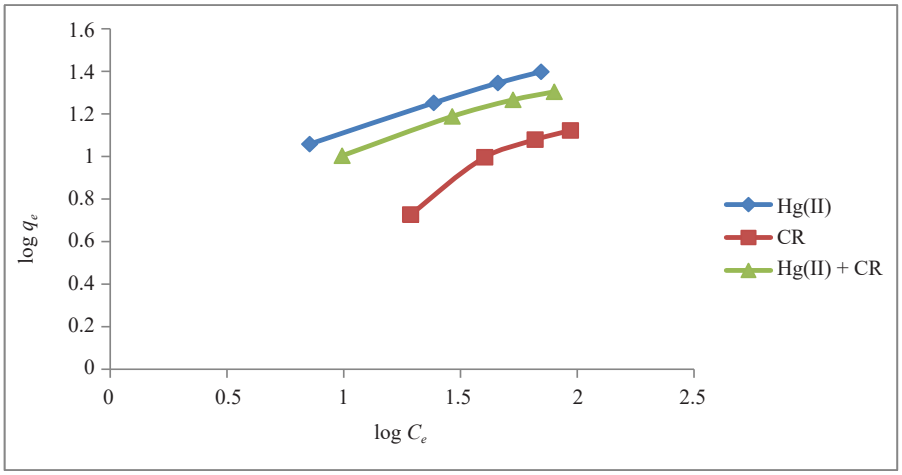

Figure 6. Freundlich isotherm plot for the sorption of mercury (II) ions, Congo red dye and their binary mixture onto modified mango leaves. Hg (II) = Mercury (II) ion and CR = Congo red dye and Hg (II) + CR = mercury (II) ions and Congo red dye

Figure 6 shows a straight-line graph following the Freundlich isotherm model, used to describe the sorption of Hg^{2+} ions, Congo red dye, and their binary mixture onto modified mango leaves. Typically, this model involves plotting log q_e against log C_e to evaluate the sorption characteristics.

Table 3. Freundlich isotherm parameters

Mercury (II) ions		Congo red dye		Binary mixture	
N	K_F	N	K_F	N	K_F
2.890	5.84	1.724	1.026	2.976	4.764

The outcomes illustrated in Table 3 demonstrate that the equilibrium data concerning the adsorption of mercury (II) ions, Congo red dye, and their combination are most accurately represented by the Freundlich isotherm model. This deduction is based on the array of N-values and R^2 values, which closely approximate unity. As outlined by Chen et al.[35] N-values ranging from 2 to 10 indicate favorable sorption attributes, whereas values between 1 and 2 suggest moderate sorption, and values below 1 imply less efficient sorption. It is noteworthy that the sorption intensity (N) value for the combined mixture is the highest, standing at N = 2.976, signifying that the Freundlich isotherm model is the most appropriate fit for the sorption of the binary mixture of Congo red dye and mercury (II) ions employing modified mango leaves. In this mechanism, a multi-layer is established through physico-sorption adsorption, aligning with earlier investigations.[36-37]

By way of illustration, the adsorption of Acid Red 88 dye and Ni (II) ions utilizing a natural adsorbent sourced from sugarcane bagasse was most effectively expounded by the Freundlich isotherm.[38] Correspondingly, the adsorption of Pb (II) ions and Basic Red 46 dye onto magnetic graphene oxide also adhered to the Freundlich isotherm, as indicated by Liu et al.. In an examination by Kumar et al.[39] the adsorption of Congo red dye from aqueous solution utilizing Neem leaf powder was observed to align well with the Freundlich isotherm. Furthermore, the researchers noted that the N value derived for Congo red dye adsorption fell within the favorable range of 1 to 10, denoting a beneficial adsorption procedure. On the whole, the utilization of the Freundlich isotherm to simulate the adsorption of heavy metals and dyes by diverse adsorbents, coupled with the establishment of multilayer adsorption in such procedures, has been extensively documented in scholarly works.

3.2.3 *Brunaer-Emette-Teller*

The BET derived an adsorption isotherm based on assumption that the adsorbate molecules could be adsorbed in more than one layer thickness on the surface of adsorbent. The BET model can be expressed as:

$$C_e/(C_s - C_e)\, q_e = 1/K_b q_m + K_b - 1/K_b q_m\, (C_e/C_s) \quad (2)$$

This is a plot of $C_e/(C_s - C_e)q_e$ against C_e/C_s that gives a straight line with slope of $K_b - 1/K_b q_m$ and intercept of $1/K_b q_m$.

Table 4. Brunaer-Emette-Teller isotherm parameters

Mercury (II) ions		Congo red dye		Binary mixture	
q_m	K_b	q_m	K_b	q_m	K_b
0.0096	-0.66	0.015	-3.45	0.047	-2.287

The data presented in Table 4 demonstrate that the sorption of mercury (II) ions, Congo red dye, and their combination is most accurately explained by the BET isotherm model, as evidenced by the thorough analysis of the regression coefficients. It is of particular note that mango leaves treated with potassium persulfate display the highest adsorption capacity for Congo red dye (q_m = 0.015 mg/g), surpassing capacities for mercury (II) ions (q_m = 0.0096 mg/g) and their combination (q_m = 0.047 mg/g). This observation implies that the BET isotherm model is most appropriate for elucidating the sorption of Congo red dye, suggestive of a physico-sorption adsorption mechanism.

These results mirror earlier studies on the effective removal of Congo red dye utilizing various adsorbents, such as modified agricultural residues like mango leaves. For instance, Abechi et al.[40] documented the successful removal of Congo red dye with mango leaves modified using sodium hydroxide, achieving a higher adsorption capacity of 12.24 mg/g. In contrast, Rahman et al.[41] explored chitosan-coated kaolin as an adsorbent, reporting a notably higher adsorption capacity of 20.5 mg/g. Nevertheless, chitosan-coated kaolin represents a synthetic adsorbent, which may be less economically and environmentally advantageous compared to natural waste adsorbents.

The utilization of potassium persulfate to modify mango leaves has been previously investigated by Abechi et al.[40] who observed an enhanced adsorption capacity for Congo red dye, indicating improved surface characteristics due to chemical alteration. In general, these outcomes are in agreement with prior studies on natural waste adsorbents and chemical modification methodologies for the elimination of Congo red dye.

3.3 *Adsorption kinetics*

Adsorption kinetics provides the information about the mechanism of adsorption which is important for efficiency of the adsorption process.

3.3.1 *Lagergren (pseudo) first order model*

This study focuses on the graph of the natural logarithm of the difference between q_e and q_t plotted against time t, where the constants K_1 and q_e are determined based on the gradient and y-intercept of the graph. The graphical representation in Figure 7 illustrates the relationship described by the pseudo first-order model, specifically at a concentration level of 120 mg/L and various time points (10, 15, 20, 25 minutes).

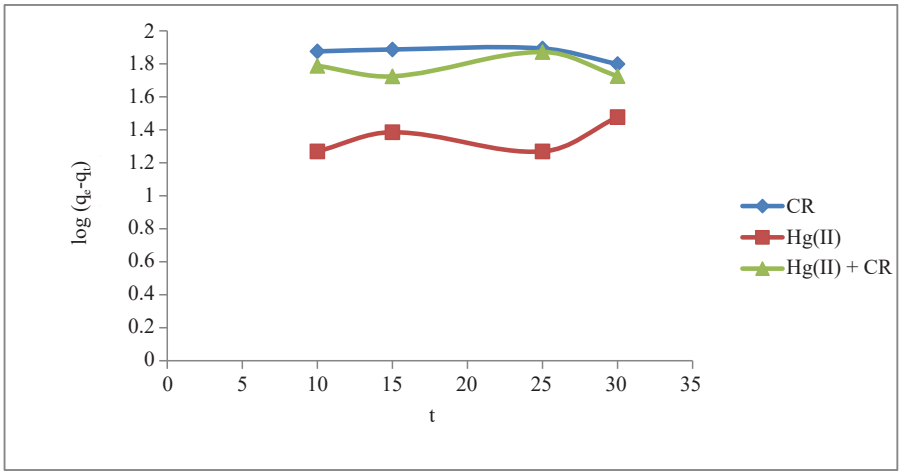

Figure 7. Plot of pseudo first order model of the adsorption of mercury (II) ions, Congo red dye and their binary mixture onto modified mango leaves. pH = 7, Initial concentration = 120 mg/L, Agitation speed = 100 rpm, Adsorbent dosage = 0.1 g, Hg (II) = Mercury (II) ions and CR = Congo red dye and Hg (II) + CR = mercury (II) ions and Congo red dye

Table 5. Pseudo First order Kinetic Parameters for the adsorption of mercury (II) ions, Congo red dye and their binary mixture by modified mango leaves

Parameters	Mercury (II) ions	Congo red dye	Binary mixture
q_e exp (mg/g)	71.45	96.45	91.235
q_e cal (mg/g)	17.08	85.76	58.28
K_1 (min^{-1})	-0.0136	0.0074	-0.0136

3.3.2 *Pseudo second order model*

The pseudo-second order kinetic rate equation was expressed as[41]

$$dq_t/dq_t = k_2(q_e - q_t)^2 \quad (3)$$

$$t/qt = 1/k_2q_e2 + 1/q_et \quad (4)$$

This is the plot of t/q_t against t in which q_e and K_2 are calculated from the slope and intercept respectively from the plot.

Figure 8 shows the plot of pseudo second order model at concentration of 120 mg/L and at varied time (10, 15, 20, 25, 30 minutes).

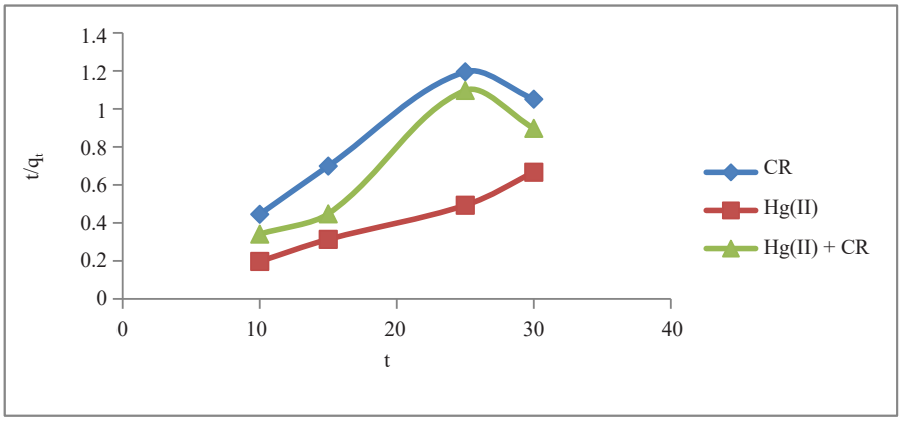

Figure 8. Plot of pseudo second order model of the adsorption of mercury (II) ions, Congo red dye and their binary mixture onto modified mango leaves. pH = 7, Initial concentration = 120 mg/L, Agitation speed = 100 rpm, Adsorbent dosage = 0.1 g, Hg (II) = Mercury (II) ion and CR = Congo red dye and Hg (II) + CR = mercury (II) ions and Congo red dye

Table 6. Pseudo second order Kinetic Parameters for the adsorption of mercury (II) ions, Congo red dye and their binary mixture by modified mango leaves

Parameters	Mercury (II) ions	Congo red dye	Binary mixture
q_e exp (mg/g)	72.45	96.37	91.238
q_e cal (mg/g)	45.455	29.50	28.45
K_2 (min^{-1})	-0.0016	0.0063	0.136

The selection of equilibrium kinetics is contingent upon the alignment of experimental and calculated q_e values.

Upon comparing the data presented in Tables 5 and 6, it became apparent that the Pseudo First Order kinetics proved to be the most appropriate model for the adsorption of Congo red dye and its binary mixture onto modified mango leaves. This determination was based on the close correspondence observed between the calculated and experimental equilibrium adsorption capacity values within the framework of Pseudo First Order kinetics, as opposed to Pseudo Second Order kinetics. Conversely, the Pseudo Second Order kinetics was identified as the most suitable model for the adsorption of mercury (II) ions onto modified mango leaves. In this case, the calculated equilibrium adsorption capacity closely approximated the experimental value within the context of Pseudo Second Order kinetics, diverging from Pseudo First Order kinetics.

These observations are consistent with previous studies on adsorption kinetics, where the choice of the appropriate model relies on the specific characteristics of the adsorbent and adsorbate system. For example, Wang et al.[9] demonstrated the suitability of Pseudo Second Order kinetics for fluoride ion adsorption onto magnetic graphene oxide, while Pseudo First Order kinetics proved effective for malachite green dye adsorption onto the same adsorbent. Similarly, Nethaji et al.[42] noted that Pseudo Second Order kinetics was fitting for chromium ion adsorption onto tannery waste, while Pseudo First Order kinetics was deemed appropriate for crystal violet dye adsorption onto the same adsorbent.

These findings indicate that the adsorption kinetics of Hg^{2+}, Congo red dye, and binary mixtures onto modified mango leaves can be accurately explained by employing the Pseudo Second Order kinetic rate equation for mercury (II) ions and the Pseudo First Order kinetic rate equation for Congo red dye and its binary mixture. Such insights carry significant implications for the development of more efficient and effective adsorption systems aimed at removing pollutants from wastewater and other contaminated sources.

3.3.3 *Intraparticle diffusion model*

The model addresses the step that limits the rate, formulated as;

$$q_t = Kt^{1/2} + C \tag{5}$$

This graph elucidates the correlation between "q_t" and "t", where the data points create linear patterns originating from the origin. The gradient of these patterns offers insights into the constant of intra-particle diffusion rate (Kid), while the intersection at the origin signifies the constant C. Figure 9 showcases this model of intra-particle diffusion graph at a concentration of 120 mg/L, with measurements conducted at different time intervals (10, 15, 20, 25, and 30 minutes).

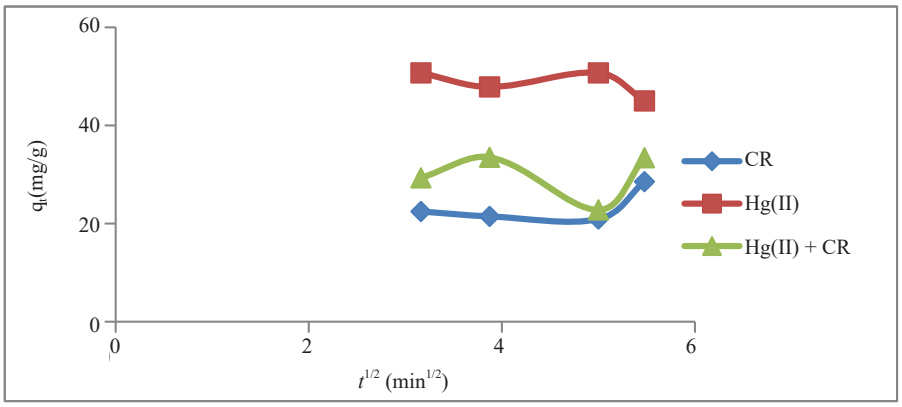

Figure 9. Plot of intraparticle diffusion model of the adsorption of mercury (II) ions, Congo red dye and their binary mixture onto modified mango leaves. pH = 7, Initial concentration = 120 mg/L, Agitation speed = 100 rpm, Adsorbent dosage = 0.1 g, Hg (II) = Mercury (II) ion and CR = Congo red dye and Hg (II) + CR = mercury (II) ions and Congo red dye

Table 7. Intra-particle diffusion model of Congo red dye, mercury (II) ions and their binary mixture by modified mango leaves

Parameters	Mercury (II) ions	Congo red dye	Binary mixture
K_{id}	-1.453	1.872	-0.5
C	54.93	15.14	31.94
R^2	0.313	0.313	0.01

The outcomes derived from the intra-particle diffusion model as shown in Table 7, demonstrate that the adsorption mechanism of mercury (II) ions, Congo red dye, and their combined mixture onto modified mango leaves did not strictly conform to this particular model. This deviation is apparent as the plots of q_t versus t do not originate from a common point, indicating that the intra-particle diffusion alone was not the predominant factor influencing the rate-controlling step. Moreover, the inadequate correlation coefficients (R^2) imply a substandard fitting of the model to the empirical data, which is in line with observations from prior research. For example, previous studies, such as that of Moyo and Onyango,[43] have shown similar inconsistencies with the intra-particle diffusion model in the context of chromium (VI) adsorption on activated carbon from sugarcane bagasse.

When examining the intra-particle diffusion rate constant (K_{id}) and the constant (C) in the context of adsorbing mercury (II) ions, Congo red dye, and their binary mixture, it was observed that the constant value for Congo red dye surpassed the others. This observation indicates that the process of intra-particle diffusion significantly impacted the adsorption of Congo red dye onto modified mango leaves, which aligns with the findings of studies such as Baral et al.[44-45] on the adsorption of methylene blue on banana stems and sheaths.

Nonetheless, although intra-particle diffusion played a significant role in the adsorption of Congo red dye, it was not the sole governing factor in the adsorption process of mercury (II) ions, Congo red dye, and their binary mixture. Further research is necessary to comprehensively comprehend the underlying mechanisms driving adsorption and to optimize the conditions for enhanced adsorption efficacy.

3.4 *Thermodynamics of adsorption*

The study explores the thermodynamics of adsorption onto modified powdered mango leaves, assessing the spontaneity and feasibility through Gibbs free energy change ($\Delta G°$). Negative $\Delta G°$ values (-9.42 kJ/mol for mercury (II) ions and -8.71 kJ/mol for Congo red dye) indicate spontaneity under the experimental conditions. Enthalpy change ($\Delta H°$) values (+18.56 kJ/mol for mercury (II) ions and +22.08 kJ/mol for Congo red dye) suggest endothermic adsorption, requiring heat absorption. Positive entropy change ($\Delta S°$) values (+80.36 J/(mol·K) for mercury (II) ions and +91.94 J/(mol·K) for Congo red dye) indicate increased disorderliness during adsorption. The Van't Hoff equation relates equilibrium constant (K) to temperature (T), $\Delta H°$, and $\Delta S°$, affirming thermodynamic stability with negative $\Delta G°$ alongside positive $\Delta H°$ and $\Delta S°$. These findings collectively support the favourable and effective adsorption of mercury (II) ions and Congo red dye onto modified mango leaves.

4. Conclusion

The study effectively demonstrates the potential of using modified powdered mango leaves treated with potassium persulfate to remove Congo red dye, mercury (II) ions, and their binary mixtures from polluted wastewater. It aimed to address the elimination of both organic and inorganic pollutants through adsorption onto the modified mango leaves. The research employs thorough experimental methodologies, assessing and enhancing various factors influencing the adsorbent's efficacy. Kinetic information gathered for Congo red dye and its binary mixture aligns well with the pseudo (Lagergren) first-order model, while mercury (II) ions' adsorption kinetics conform to the pseudo-second-order model. Notably, the study emphasizes the significant influence of pH on Congo red dye adsorption, identifying optimized conditions for potentially cost-efficient and eco-friendly treatment processes. By highlighting the effectiveness of

modified agricultural waste materials, such as powdered mango leaves, in pollutant removal, the study introduces a novel approach to wastewater treatment. It underscores the importance of exploring eco-friendly and economically viable solutions and contributes to the development of sustainable methodologies for addressing water pollution challenges.

Conflict of interest

Authors declare there is no conflict of interest at any point with reference to research findings.

References

[1] Chen, Z.; Wu, L.; Liu, Y. *J. Hazard. Mater*. **2020,** *384*, 121254.
[2] Gupta, V. K.; Nayak, A.; Agarwal, S. *J. Mol. Liq*. **2020,** *314*, 113888.
[3] Wang, J.; Zhang, X.; Wang, L. *J. Environ. Manage*. **2021,** *284*, 112013.
[4] Ahmad, R.; Nafees, M.; Hashmi, M. *Rev. Chem. Eng*. **2021,** *37*(3), 601-624.
[5] Islam, M. S.; Saha, B. B.; Sikder, M. T. *J. Environ. Chem. Eng*. **2019,** *7*(6), 103512.
[6] Deshmukh, S.; Topare, N. S.; Raut-Jadhav, S.; Thorat, P. V.; Bokil, S. A.; Khan, A. *Ecosystems Soc*. **2022,** *71*(12), 1351.
[7] Liu, X.; Lin, Z.; Zhang, Y. *J. Environ. Manage.* **2021,** *292*, 112705.
[8] Muhulet, A.; Iordache, A.; Miricioiu, M. G. *J. Environ. Chem. Eng.* **2021,** *9*(3), 105352.
[9] Wang, Y.; Wu, J.; Xu, Y.; Zhou, K.; Zhang, H.; Guo, S. *Water Sci. Technol.* **2021,** *84*(7), 1563-1574.
[10] Devi, N.; Saroha, A. K. *J. Environ. Chem. Eng.* **2021,** *9*(3), 105384.
[11] Fazlzadeh, M.; Rostami, R.; Shirzad-Siboni, M. *J. Cleaner Prod.* **2021,** *315,* 128074.
[12] Kumar, N. S.; Kumar, P. S. *J. Environ. Chem. Eng.* **2021,** *9*(4), 105620.
[13] Sun, G.; Liu, Y.; Xue, Y. *Mater.* **2018,** *11*(2), 193.
[14] Xue, Y.; Gao, X.; Yao, Y.; Wang, X.; Zhu, F. *Chem. Eng. J.* **2016,** *283*, 1206-1213.
[15] Isah, A. D.; Ibrahim, M. A. *J. Environ. Chem. Ecotoxicol.* **2019,** *11*(3), 24-34.
[16] Sathya, M.; Gnanasambandan, T.; Arivoli, S. *J. Environ. Chem. Eng.* **2017,** *5*(6), 6106-6116.
[17] Liu, Y.; Zhang, Y.; Li, J.; Li, Q.; Chen, C.; Huang, H. *J. Mol. Liq.* **2018,** *269*, 534-542.
[18] Hu, Q.; Zhang, L.; Li, Y.; Chen, J.; Wei, Y. *Carbohydr. Polym.* **2018,** *194*, 1-15.
[19] Rustamaji, H.; Prakoso, T.; Devianto, H.; Widiatmoko, P.; Kurnia, K. A. *Bioresour. Technol. Rep.* **2023,** *21*, 101301.
[20] Chakraborty, S.; Saha, P. D.; Chowdhury, S. *Int. J. Environ. Sci. Technol.* **2013,** *10*(5), 999-1008.
[21] Pham, T. H. *Non-Met. Sci.* **2023,** *05*(01), 1-11.
[22] Akhlaq, A.; Malik, R. N.; Ghauri, M. A. *J. Chem. Soc. Pakistan.* **2016,** *38*(5), 904-914.
[23] Bhattacharya, A. K.; Ray, S. K. *Appl. Clay Sci.* **2019,** *171*, 42-56.
[24] Adelaja, O.; Keshavarz, T.; Kyazze, G. *Int. Biodeterior. Biodegrad.* **2017,** *11*(6), 91-103.
[25] Ong Pick Sheen. *J. Environ. Sci. Technol.* **2011,** *4*(4), 419-428.
[26] Gupta, V. K.; Ali, I.; Suhas; Mohan, D. *J. Colloid Interface Sci.* **2003,** *265*, 257-264.
[27] Cheng, Y.; Yang, Z.; Wang, H.; Wang, M.; Hu, X.; Ding, X. *J. Mol. Liq.* **2016,** *219*, 672-679.
[28] Lu, J.; He, X.; Chen, D.; Sun, S.; Cai, Z.; Liu, Y. *Environ. Sci. Pollut. Res.* **2016,** *23*(6), 5244-5254.
[29] Sharma, Y. C.; Uma, S.; Upadhyay, S. N. *J. Chem. Pharm. Res.* **2010,** *2*(2), 165-176.
[30] Wang, J.; Zheng, Y.; Zhou, Y.; Wang, A.; Zheng, Y. *Int. J. Biol. Macromol.* **2018,** *118*, 972-979.
[31] Gebremedhin, G. *Int. J. Mod. Chem. Appl. Sci.* **2016,** *3*(2), 369-377.
[32] Zhou, Y.; He, J.; Chen, R.; Li, X. *Mater. Today Sustain*. **2022,** *18*, 100138.
[33] Wang, X.; Lu, Y.; Yu, H.; Ma, X.; Chen, X. *J. Environ. Manage.* **2020,** *261*, 110252.
[34] Khan, T. A.; Khan, E. A.; Asiri, A. M. *Desalination.* **2011,** *265*(1-3), 126-134.
[35] Chen, Y.; Guo, J.; Zhang, S.; Shen, Y.; Li, C. *J. Hazard. Mater.* **2010,** *181*(1-3), 554-562.
[36] Rashid, M. H. O.; Islam, M. S.; Islam, M. J.; Islam, M. A.; Islam, M. S.; Karim, M. R. *Desalin. Water Treat.* **2019,** *145*, 34-44.
[37] Fawzy, M.; Taha, R.; Khedr, S. *Environ. Technol. Innov.* **2019,** *15*, 100406.
[38] Liu, Y.; Zhou, W.; Zhang, Y.; Zhang, B.; Huang, H. *Bioresour. Technol.* **2019,** *287*, 121436.

[39] Kumar, A.; Prasad, B.; Mishra, I. M.; Chand, S. *J. Environ. Chem. Eng.* **2016,** *4*(3), 3089-3101.
[40] Abechi, S. E.; Gimba, C. E.; Yusuf, H. M.; Umar, I. A. *J. Environ. Chem. Eng.* **2018,** *6*(4), 4404-4414.
[41] Ho, Y. S.; Mckay, G. *Process Biochem.* **1998,** *34*, 451-465.
[42] Rahman, M. A.; Binti Alias, N.; Halim, N. A. Rev. *J. Cleaner Prod.* **2021,** *278*, 123798.
[43] Nethaji, S.; Venkatachalam, R.; Ramalingam, S.; Sundaram, M. M. *J. Environ. Chem. Eng.* **2022,** *10*(1), 106124.
[44] Moyo, M.; Onyango, M. S. *J. Environ. Chem. Eng.* **2015,** *3*(1), 97-110.
[45] Baral, S.; Das, S. N.; Roy, S.; Bhattacharyya, K. G. *Desalination Water Treat.* **2013,** *51*(25-27), 4886-4899.